NARR's Atmospheric Water Cycle Components. Part II: Summertime Mean and Diurnal Interactions

ALEX C. RUANE

NASA Goddard Institute for Space Studies, and NASA/Oak Ridge Associated Universities Postdoctoral Program, and Sigma Space Partners LLC, New York, New York

(Manuscript received 8 February 2010, in final form 30 July 2010)

ABSTRACT

Summertime interactions in the North American Regional Reanalysis (NARR) atmospheric water cycle are examined from a user's perspective over the 1980–99 period with a particular emphasis on the diurnal cycle, the nocturnal maximum of precipitation over the Midwest, and the impacts of precipitation assimilation. NARR's full-year mean atmospheric water cycle and its annual variations are examined in Part I of this study. North American summertime (June–August) features substantial convective activity that is often organized on a diurnal scale, although diverse regional diurnal features are evident to various extents in high-resolution precipitation products. NARR's hourly assimilation of precipitation observations over the continental United States allows it to resolve diurnal effects on the water cycle, but in other regions the diurnal cycle of precipitation is imposed from an external reanalysis model. The prominent nocturnal maximum in precipitation across the upper Midwest is captured in NARR, but different precipitation assimilation sources disrupt the propagation of convective systems across the Canadian border. Normalized covariances of NARR's diurnal water cycle component interactions in the nocturnal maximum region reveal a strong relationship between moisture convergence and precipitation, and also measure the way in which the precipitable water column holds a lagged response between evaporation and precipitation. In many regions the diurnal cycle of rainfall is driven by interactions with water cycle components that differ from those driving the seasonal cycle. A comparison between NARR's precipitation and an estimate of the model precipitation prior to precipitation assimilation distinguishes the portion of the water cycle captured in full by the model and that which is value added by the assimilation routine. The nocturnal rainfall maximum is not present in the model precipitation estimate, leading to diurnal-scale biases in the evaporation and moisture flux convergence fields that are not directly modified by precipitation assimilation.

1. Introduction

The National Centers for Environmental Prediction (NCEP) North American Regional Reanalysis (NARR; Mesinger et al. 2006) covers one of the best-observed regions in the world, achieving new accomplishments in the range and resolution of assimilated data including a novel precipitation assimilation scheme. This effort is tremendously appealing to a wide range of users, particularly those with the need for long records of hydrometeorological variables at high spatial and temporal resolutions. NARR is suitable for many climate impacts assessments (e.g., water resources, agriculture, health, energy, etc.), which are often run on scales ranging from river catchments to local communities and require data with proper mean statistics (e.g., seasonal and longer) as well as adequate treatment of the higher-frequency climate extremes that may tip a system past key thresholds. NARR's inclusion of hourly precipitation assimilation also provides new insights into the processes affecting precipitation, which in global reanalyses are dominated by parameterization triggers that tend toward too frequent light rainfall (Trenberth et al. 2003). NARR produces impressive matches with observed precipitation on various time scales (Becker et al. 2009), but the precipitation assimilation scheme introduces discontinuities and errors that users must account for when using NARR to generate climate scenarios for impacts assessments or interpreting process studies relating to the North American hydroclimate. This study examines the North American summertime hydroclimate and its diurnal cycle to establish a framework for intercomparing

Corresponding author address: Alex C. Ruane, NASA Goddard Institute for Space Studies, 2880 Broadway, New York, NY 10025. E-mail: aruane@giss.nasa.gov

DOI: 10.1175/2010JHM1279.1

© 2010 American Meteorological Society

NARR with other datasets, to identify regions of interesting patterns of behavior for further study, and to help NARR users interpret water cycle imbalances.

As was the case in Ruane 2010 (hereafter Part I), which examined NARR's mean hydroclimate and annual component interactions, this companion study has three main parts. First NARR's summertime (June–August) water cycle is examined from 1980 to 1999, providing a 20-yr climatology of the most convective season that may serve as a basis for comparison with observations, other models, reanalysis products, climate models, and future scenarios [e.g., from the North American Regional Climate Change Assessment Program (NARCCAP); Mearns et al. (2009)]. Second, diurnal water cycle component interactions with rainfall are explored to identify key regimes that may potentially be sensitive to large-scale variability (e.g., the El Niño–Southern Oscillation, Arctic Oscillation, etc.) or climate change. Finally, to track the propagation of evident biases in the precipitation assimilation scheme throughout the water cycle, residual error terms are investigated using an estimate of the water cycle before and after precipitation assimilation occurs.

The diurnal cycle is a fundamental mode of atmospheric variability, with external solar forcing driving dynamic and thermodynamic responses that vary among regions and seasons. It is thus not surprising that many studies of the water cycle have examined the diurnal cycle in observations (e.g., Dai 2001; Nakamura 2004; Dai et al. 2007; Ruane and Roads 2007a,b), models (e.g., Dai et al. 1999; Dai and Trenberth 2004), and reanalyses (e.g., Ruane and Roads 2007a,b, 2008). Part I revealed that annual precipitation peaks in the summertime over most parts of North America east of the Rockies. The association of this maximum with peak annual evaporation suggests an environment conducive to moist thermodynamic destabilization, often realized by afternoon convective activity when the annual and diurnal solar signals combine. Wallace (1975) noted that there were some parts of North America where precipitation had distinctive diurnal phases, including a nocturnal maximum over the upper midwestern United States. These regions are affected by local and regional dynamics, governed largely by the Rocky Mountains acting as an elevated heat source as they absorb midday sunshine, initiating rising air conducive to afternoon convection but also remotely inhibiting Great Plains convection with large-scale afternoon descent. Carbone et al. (2002) tracked lines of convection originating over the lee of the Rockies and then dynamically propagating across the upper Midwest to produce the nocturnal maximum as the Rockies' mountain–lowland circulation weakened in the evening.

The diurnal scale of convection is also important in understanding extreme convective events (Trenberth et al. 2003), as well as in understanding the role of local recycling of moisture for precipitation (Anderson et al. 2009; Dirmeyer and Brubaker 2007). The summertime months were chosen for this study to emphasize diurnal convection rather than the synoptic activity that dominates during the late springtime peak in rainfall, although the interaction of diurnal circulations and upper-air synoptic conditions leads to the springtime maximum in rainfall over the central United States (Wang and Chen 2009). In many parts of the continent, the diurnal cycle is strongest when anticyclonic synoptic conditions allow local organization on a faster time scale, with convection accounting for up to 80% of warm season rainfall via thunderstorms and mesoscale convective complexes in portions of the central United States (Fritsch et al. 1986; Changnon 2001).

Simulation of the diurnal cycle is quite challenging, as the temporal and spatial scales involved in convective activity include a vast array of subgrid-scale processes. Ruane and Roads (2007a) used a global reanalysis to demonstrate that errors in the convective parameterization that accounts for these subgrid-scale processes drive overly consistent diurnal cycles over North America despite the assimilation of moisture convergence fields that properly indicate diverse regional patterns of behavior. Convective precipitation also remains a common obstacle to accurately simulating the atmospheric water budget, with errors propagating throughout the hydroclimatic system. Ruane and Roads (2008, hereafter RR2008) replaced precipitation from the NCEP–Department of Energy Reanalysis-2 (R2; Kanamitsu et al. 2002) with precipitation from an observation-based high-resolution precipitation product and revealed a close relationship between moisture flux convergence and precipitation over the North American nocturnal maximum. RR2008 showed that inadequate representation of precipitation in the global reanalysis was disrupting a tightly related water cycle; NARR's precipitation corrects this to a considerable extent.

The reaction of the reanalysis system to precipitation assimilation also sheds light on the relative strengths and weaknesses of the underlying model's convective parameterization in different regions and physical settings (Rogers et al. 2009). NARR's underlying atmospheric model (Black 1994) uses the Betts–Miller–Janjić (Janjić 1994) convective parameterization, and the biases revealed in comparison to the assimilated precipitation may be used to identify improvements to this and other convective parameterizations. NARR developers are aware of many of these challenges, but this study was motivated to provide an understanding of these processes

to researchers seeking to interpret and apply NARR output.

A brief overview of NARR, its water cycle balances, and the methods of statistical analysis that will be employed are described in the next section. Diurnal precipitation assimilation sources and interactions are considered in section 3, and section 4 discusses NARR's mean summertime balance. Section 5 evaluates the atmospheric water cycle's transient balance on a diurnal time scale, and compares component interactions with precipitation to an estimate of preassimilation interactions. A summary, discussion, and future work ideas are included in the final section.

2. NARR's atmospheric water cycle

NARR's atmospheric water cycle is driven by a combination of the underlying Eta Model (Black 1994), run at 32-km resolution with 45 η levels and a four-layer version of the Noah land surface model (Ek et al. 2003), with most observations assimilated every 3 h and precipitation assimilation on an hourly basis (Shafran et al. 2004). The precipitation assimilation scheme and general water budget are summarized briefly below and are described in more detail in Part I.

In brief, hourly precipitation simulated by the underlying Eta Model is compared to observations, with differences used to 1) modify the profile of the latent heating to drive or suppress convection to match observed totals and 2) adjust water vapor and condensate in the water column to produce a moisture profile more consistent with the modified column (Lin et al. 1999; Y. Lin 2008, personal communication). This process introduces mass imbalances, although the moisture increments (I) are stored in separate vapor (VI) and condensate (CI) terms and will be used here to approximate these water budget errors:

$$I = \mathrm{VI} + \mathrm{CI}. \tag{1}$$

NARR's water cycle (detailed in Part I) may be represented as

$$T = C + E - P + r, \tag{2}$$

where T is the tendency of the precipitable water column between successive analyses, C is the convergence of moisture flux (vapor and condensate) through the sides of the column, E is evaporation from the surface into the bottom of the column, P is precipitation falling out of the column, and r is the water cycle residual including analysis increments (Schubert and Chang 1996), precipitation assimilation increments, and remaining mass imbalances. It is also helpful to define an additional quantity, M, that estimates the precipitation produced by NARR's underlying model before precipitation assimilation adjustments:

$$M \equiv P - I. \tag{3}$$

Here, M is calculated from each 3-hourly output file and, therefore, contains three precipitation assimilation iterations rather than a continuous model precipitation estimate. We will therefore consider an approximate water balance for NARR's underlying model, replacing P in Eq. (2) with the model precipitation estimate according to Eq. (3), and rearranging to group T and I as column moisture increment terms:

$$T + I = E + C - M + r. \tag{4}$$

Part I showed that the evaporation and moisture convergence terms, which are not directly adjusted in the precipitation assimilation scheme, inherit biases from the model precipitation estimate that are important to recognize when analyzing NARR's water cycle. Each water balance holds over its long-term mean,

$$\overline{T} = \overline{E} + \overline{C} - \overline{P} + \overline{r} \quad \text{and} \tag{5a}$$

$$\overline{T} + \overline{I} = \overline{E} + \overline{C} - \overline{M} + \overline{r}, \tag{5b}$$

and among the transients at any orthogonal frequency,

$$T' = E' + C' - P' + r' \quad \text{and} \tag{6a}$$

$$T' + I' = E' + C' - M' + r'. \tag{6b}$$

To isolate the transient components of the water cycle at diurnal frequencies, NARR's 3-hourly output was passed through a broadband Fourier filter that captured the variance contained in the four diurnal periods associated with a 3-hourly dataset: the 6- (4 periods daily), 8- (3 periods daily), 12- (2 periods daily), and 24-h (1 period daily) variance bands that recreate the mean day (following RR2008). A single diurnal harmonic does not capture daily variation as well as including the higher frequencies, although the diurnal signal is strongest in most locations (followed by the semidiurnal variation). To capture minor spectral leakage that results from discrete output times of a continuous process, the nearest neighboring variance bands in the variance spectrum were captured as well (see RR2008 for more details).

The covariance of P' with each other term in Eq. (6a) is then normalized by the variance of P', and likewise for M' in Eq. (6b). The result is the following relationship, which describes 100% of the diurnal variation in P' or M' through their normalized covariance with the other water budget terms:

$$\frac{\mathrm{cov}(P', P')}{\mathrm{var}(P')} \times 100\% = \frac{\mathrm{cov}(E', P') + \mathrm{cov}(-T', P') + \mathrm{cov}(C', P') + \mathrm{cov}(r', P')}{\mathrm{var}(P')} \times 100\% = 100\% \quad \text{and} \tag{7a}$$

$$\frac{\mathrm{cov}(M', M')}{\mathrm{var}(M')} \times 100\% = \frac{\mathrm{cov}(E', M') + \mathrm{cov}[-(T' + I'), M'] + \mathrm{cov}(C', M') + \mathrm{cov}(r', M')}{\mathrm{var}(M')} \times 100\% = 100\%. \tag{7b}$$

Terms in the central portion of Eqs. (7a) and (7b) were called normalized covariances in RR2008 and are the basis of water budget analyses in both parts of this study. These normalized covariances, computed for each summer and then averaged over the 1980–99 period, indicate the percentage contribution that each water cycle component makes toward precipitation at the diurnal scale.

To assist in the interpretation of these plots, let us examine the first term in the center of Eq. (7a), which is the normalized diurnal covariance of precipitation with evaporation. If $\mathrm{cov}(E', P')/\mathrm{var}(P') = 100\%$, the variance of evaporation matches the variance of precipitation on the diurnal scale. If this term $= 0\%$, then there is no diurnal covariant relationship between evaporation and precipitation. If this term $> 100\%$, evaporation varies mostly in diurnal phase with precipitation but with a greater amplitude. If this term $< 0\%$, evaporation is out of phase with precipitation at this time scale. If this term is between 0% and 100%, then evaporation's phase or amplitude deviates from precipitation's diurnal signal and evaporation can only make a partial contribution to the moisture lost through precipitation.

When interpreting these normalized covariance terms, it is important to recognize several key caveats. First, it is difficult to separate the relative contributions of phase and amplitude in the calculation of covariance (and thus normalized covariance). Second, dividing by the variance of the precipitation term can lead to very large normalized covariances in regions with low diurnal precipitation variance (typically dry areas and, notably, including portions of southern California that receive most of their rainfall in the wintertime). Third, the high frequencies examined in this study could reveal true features at fine spatial resolution, but features that are consistent across several grid boxes in NARR are likely more robust. Finally, it is important to remember that the diurnal component interactions exist on top of mean interactions and variations on different time scales, so these diurnal patterns of behavior may counteract more prevalent patterns of behavior in any given location. The scope of this study is too large to analyze each of the features identified, but while covariation cannot be mistaken for causation, normalized covariances can help identify patterns of water cycle behavior and it is hoped that these results will encourage additional analyses to determine precise causation.

3. Diurnal precipitation assimilation sources and interactions

Precipitation assimilation heavily influences NARR's diurnal cycle and has an inherent diurnal cycle of its own. Table 1 shows the source of the observations for precipitation assimilation in each region, as well as its frequency and temporal downscaling (based upon Shafran et al. 2004). In general, the diurnal cycle that is ingested by the precipitation assimilation as "observations" is necessarily of lower quality than the raw observations. The

TABLE 1. Overview of the precipitation assimilation for each region of the NARR (based upon Shafran et al. 2004). The datasets from which the precipitation is taken for assimilation, the frequency of precipitation measurements from that source, and the source from which higher-frequency values are drawn to fill in the gaps are shown in columns 2–4. The R2 output, which was used as high-frequency filling for several regions, was taken from hourly forecasts from the 12–24-h forecasts initiated at 0000 and 1200 UTC.

Region	Assimilation source	Frequency of source measurements	Higher-frequency filling
Continental United States	1/8° rain gauge analysis with the Parameter-Elevation Regressions on Independent Slopes Model (PRISM)	Daily	2.5° hourly analysis
Canada	1° rain gauge analysis	Daily	~1.9° R2 forecast
Mexico	1° rain gauge analysis	Daily	~1.9° R2 forecast
Caribbean Islands and Central America	2.5°CMAP precipitation analysis	Pentad	~1.9° R2 forecast
Alaska	None	None	None
Oceans (south of 27.5° latitude)	2.5°CMAP precipitation analysis	Pentad	~1.9° R2 forecast
Oceans (27.5°–42.5° latitude)	2.5°CMAP precipitation analysis to south blended with no assimilation to north	Pentad	~1.9° R2 forecast
Oceans (north of 42.5° latitude)	None	None	None

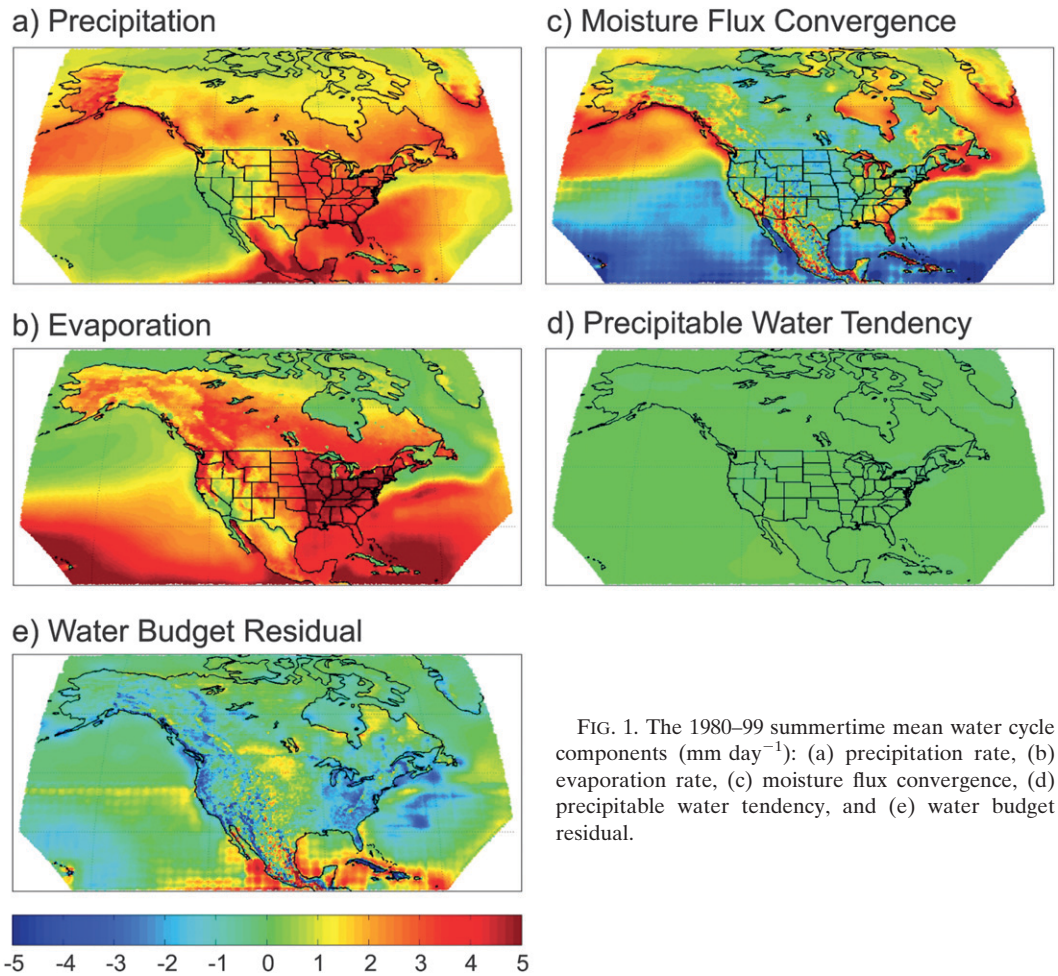

FIG. 1. The 1980–99 summertime mean water cycle components (mm day^{-1}): (a) precipitation rate, (b) evaporation rate, (c) moisture flux convergence, (d) precipitable water tendency, and (e) water budget residual.

high-resolution (1/8°) gauge dataset that covers the continental United States only contains daily values (Higgins et al. 2000), with hourly values analyzed at 2.5° (or 1/400th the spatial resolution). Daily gauge observations also drive precipitation assimilation over Canada and Mexico, while the Climate Prediction Center (CPC) Merged Analysis of Precipitation (CMAP; Xie and Arkin 1997) 5-day totals are used over oceans south of 42.5°N and land south of Mexico.

Outside of the continental United States the diurnal cycle is imposed from hourly output of 12–24-h forecasts of the R2 initialized at 0000 and 1200 UTC (W. Ebisuzaki 2009, personal communication). These longer forecasts reduce spinup or spindown errors, and differ from standard R2 diurnal cycles, which are formed from 0–6-h forecasts. As in other global reanalyses, diurnal precipitation in the R2 has an overly consistent phase and weak intensity (Trenberth et al. 2003; RR2008). The R2 utilizes the simplified Arakawa–Schubert convective parameterization (Pan and Wu 1995) and the two-layer Oregon State University land surface model (Pan and Mahrt 1987), which lead to a quick trigger in atmospheric convection during North American summers (Ruane and Roads 2007a). Several changes to this system occurred when NARR went operational in 2003 (data not analyzed in this study), and it now incorporates higher-resolution precipitation information from the CPC's morphing technique (CMORPH; Joyce et al. 2004) but does not assimilate precipitation over Canada or the oceans (W. Ebisuzaki 2009, personal communication).

4. 20-yr mean summertime balance

The 1980–99 summertime means of each NARR water cycle component are displayed in Fig. 1, as expressed in Eq. (5a). These maps reveal the water cycle balance averaged across all frequencies of variation. A subset of the NARR domain is shown in order to focus detail on the North American continent.

Summertime precipitation (Fig. 1a) is heavier than the annual mean precipitation over much of the continent (as shown in Part I) and it bears the regional effects

of different precipitation assimilation sources. On the annual average, the totals are highest over the eastern United States, but in the summertime rainfall is comparable all the way out to the foothills of the Rockies. The western mountain ranges north of Mexico, which receive most of their precipitation when wintertime synoptic systems are forced to interact with steep terrain, are drier in the summer. Mo et al. (2005) noted the stark precipitation signal at the northern and southern borders of the United States, where blending of precipitation assimilation results from differing observational sources (see Table 1) leads to local minima. The effects of precipitation assimilation are also clear over the open oceans, where precipitation is heavy over the warm southern Atlantic but discontinuously increases north of 42.5°N. The cold cyclonic gyres of the North Pacific and Atlantic continue to produce synoptic activity during the summertime, but NARR's assimilation of CMAP precipitation data ceases at this latitude. Despite these issues, NARR does closely represent the mean summertime precipitation over North America, indicating that significant value was added with the increase in resolution and precipitation assimilation.

Evaporation (Fig. 1b) is generally strong during the summertime, although regional variations are evident. One exception is the North Pacific and Atlantic Oceans, where low evaporation in the summertime is likely due to a reduced meridional temperature gradient and a weak contrast between the ocean surface and overlying air masses (especially over the Atlantic, where air masses may retain their continental characteristics hundreds of kilometers out to sea; RR2008). As changes in the precipitable water column over the summertime are small compared to precipitation and evaporation fluxes, the difference between the precipitation and evaporation fields over land should be matched almost entirely by surface and groundwater runoff. A strong balance exists between the evaporation and precipitation fields, but evaporation exceeds precipitation over much of the continent. As NARR precipitation is constrained by precipitation assimilation, this unlikely feature must be due to an apparent high evaporation bias. The U.S.–Canadian border effect that was seen in the mean precipitation field is also apparent for evaporation. Surprisingly, evaporation over the U.S. side of the border is consistently higher than over the Canadian side. These biases, which will be further analyzed below, are similar to those identified in Part I and suggest that precipitation assimilation errors may be passed on to other portions of the water cycle.

Summertime moisture flux convergence (Fig. 1c) has large regional variation, and is reduced over much of the continent in comparison to the annual mean. The strong moisture flux convergence over the western mountains that characterizes the annual mean fields is absent in the summertime, although moisture flux convergence dominates the dynamical North American monsoon region in western Mexico and the U.S. southwest (Becker and Berbery 2008). As a result of the negative P–E bias noted above, large portions of the continental interior act as a source of summertime moisture (especially over the Missouri River basin). Moisture flux convergence is prominent over Florida, corresponding to a local maximum in precipitation and a relative reduction in evaporation. Oceanic moisture flux convergence shows the recognizable pattern of divergence over warm waters providing moisture that converges over cool northern gyres and the continents. NARR produces an interesting area of summertime convergence west of Bermuda, which is apparently related to a local minimum of sea surface temperature bounded by the warmer Gulf Stream to the west and north. The bull's-eye pattern of moisture flux convergence over the oceans is due to interpolation errors introduced by the assimilation of CMAP precipitation (Bukovsky and Karoly 2007).

The mean precipitable water tendency (Fig. 1d) is negligible over the summertime period, as fluxes into and out of the water column during this time are much larger than any net changes in the column reservoir. Due to a net warming in most locations, precipitable water tends to increase over the summer months, but the small positive values are negligible in the mean balance.

The summertime water budget residual (Fig. 1e) is greatest in locations where NARR's underlying model has difficulty, and suggests that the summertime hydrologic cycle is overactive aside from precipitation. A prominent analysis increment, common to all reanalysis systems, is present over mountainous areas where complex terrain prevents a match with the coarser model grid. The large residuals away from the mountains (where the analysis increment is reduced) are due to an imbalance between precipitation, evaporation, and moisture flux convergence. Solving for $\bar{r}$ in Eq. (5a), a negative water budget residual may only come from an underestimate of precipitation or an overestimate of the evaporation and/or moisture flux convergence terms (recognizing that the precipitable water tendency is negligible), and the opposite is true for a positive residual. Precipitation assimilation is constrained by assimilated observations, so these biases are likely due to an over- or underestimate of the other terms. The geographical pattern of the negative biases generally matches the mean evaporation field, indicating that these biases are largely the result of overestimated evaporation. The positive residuals seem to match the areas of summertime moisture flux divergence, suggesting that NARR overestimates the continental moisture source. The mean summertime biases in the

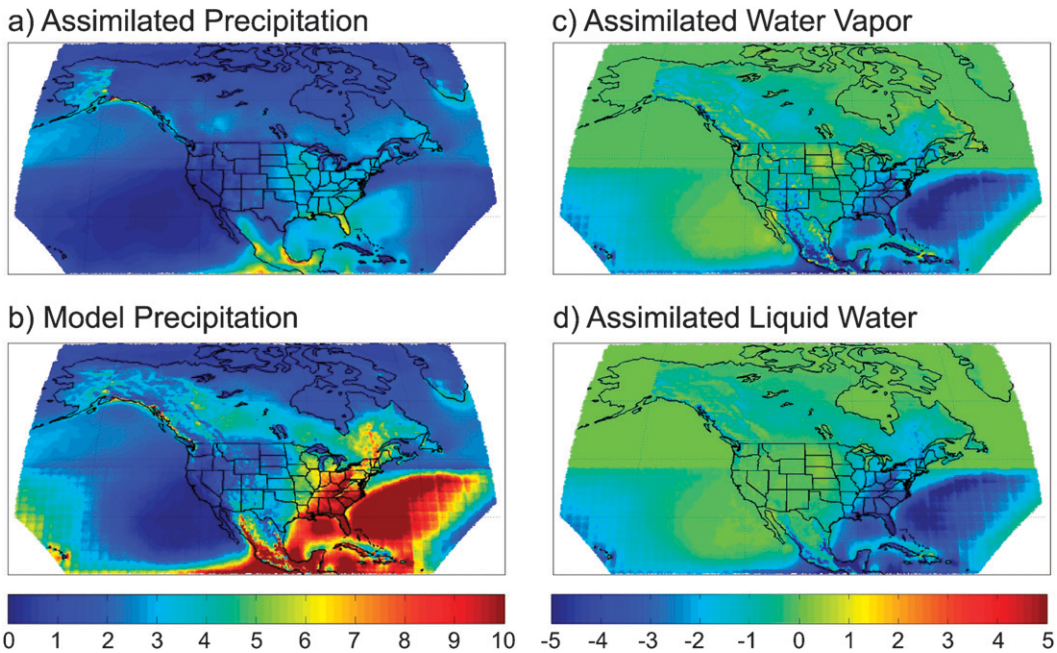

FIG. 2. The 1980–99 summertime mean precipitation assimilation components (mm day^{-1}): (a) assimilated precipitation rate, (b) model precipitation rate, (c) assimilated water vapor, and (d) assimilated liquid water. Note that the color bars for the precipitation terms in (a) and (b) are different from the color bars for the assimilation terms in (c) and (d).

evaporation and moisture convergence field suggest that they are following a more active hydrologic cycle than is precipitation, as was noted in Part I.

To investigate the strength of the underlying model's hydrologic cycle, mean summertime components of precipitation assimilation [according to Eq. (3)] are presented in Fig. 2. The precipitation assimilation process tends to reduce North American summertime rainfall (with the notable exception of the upper midwestern United States), leaving overestimates of evaporation and moisture flux convergence that are not adjusted (as suggested by Nigam and Ruiz-Barradas 2006; Kanamaru and Kanamitsu 2007; West et al. 2007; Part I). NARR precipitation (Fig. 2a) is much lower than the estimate of model precipitation before assimilation (Fig. 2b), particularly over the eastern United States. Precipitation assimilation also greatly reduces excessive model precipitation over Texas, New Mexico, the western Atlantic, and much of Canada. The precipitation assimilation scheme adjusts both water vapor (Fig. 2c) and liquid water (Fig. 2d), but strongly favors vapor increments over the western United States and North American monsoon region in Mexico. The upper Midwest is nearly the only location where precipitation assimilation increases the precipitation amount reported in NARR, relying on mostly vapor increments and likely underestimating evaporation and moisture flux convergence (the same is true for a small region in the Gulf of California). The upper Midwest will be particularly focused on in the next section.

5. Diurnal balance

a. Diurnal harmonics

Hourly precipitation and radiation assimilation, along with 3-hourly atmospheric state assimilation, allows NARR to capture a high degree of the water cycle's diurnal variability. These assimilated quantities only directly affect the diurnal cycle of the precipitation and precipitable water tendency components, however, relying on internal model dynamics, thermodynamics, and parameterization sets to simulate the diurnal variations of evaporation and moisture flux convergence. The normalized covariance of each water cycle component with diurnal precipitation is examined in this section to analyze the highly constrained diurnal water cycle, but also to identify NARR regions where budget errors persist.

Figure 3 explores the diurnal precipitation variation that forms the basis of these normalized covariance examinations, comparing a simple diurnal harmonic of NARR precipitation to the global R2 and two high-resolution precipitation products (HRPPs). These HRPPs (briefly described in Ruane and Roads 2007b), CMORPH

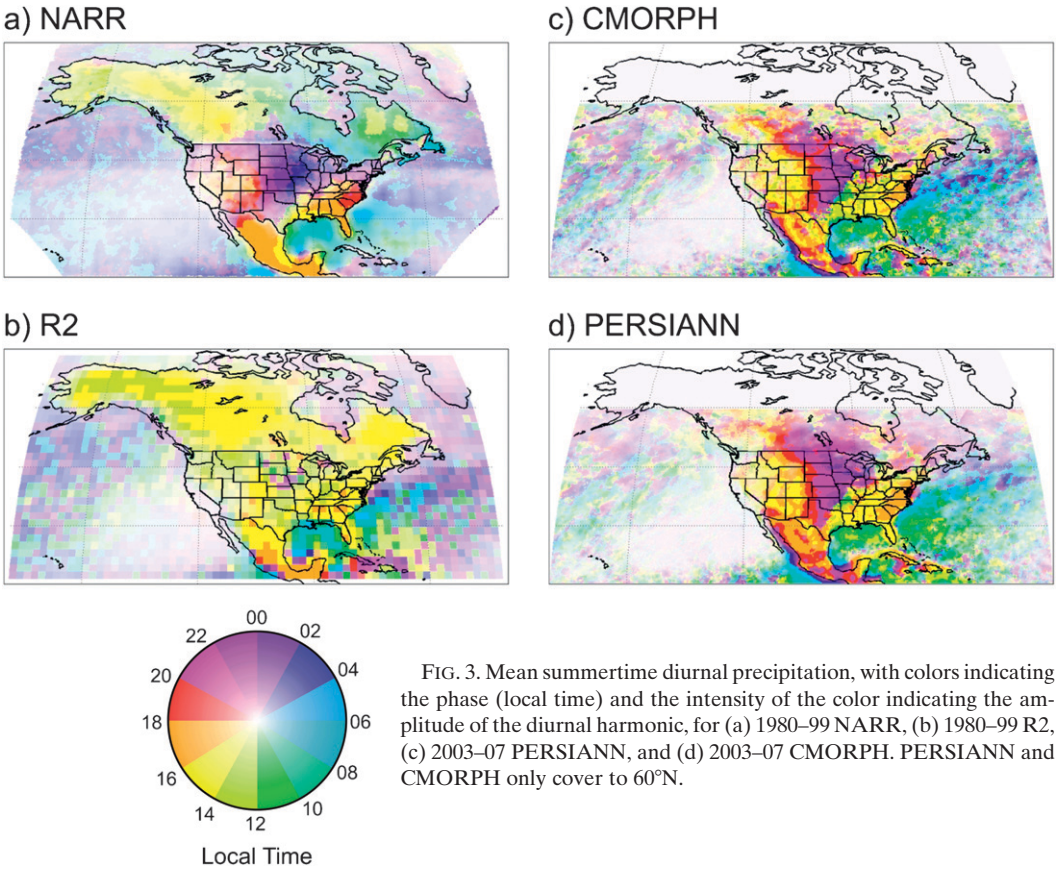

FIG. 3. Mean summertime diurnal precipitation, with colors indicating the phase (local time) and the intensity of the color indicating the amplitude of the diurnal harmonic, for (a) 1980–99 NARR, (b) 1980–99 R2, (c) 2003–07 PERSIANN, and (d) 2003–07 CMORPH. PERSIANN and CMORPH only cover to 60°N.

(Joyce et al. 2004) and the Precipitation Estimation Using Remotely Sensed Information and Artificial Neural Networks product (PERSIANN; Hsu et al. 1997), use a combination of polar-orbiting instruments and ground-based rainfall measurements to train geostationary satellite information to pick up rainfall rates with nearly global coverage equatorward of 60°N–S latitude. The diurnal HRPP errors introduced by the use of microwave measurements over land may also be explored through comparisons with the diurnal cycle of NARR's assimilated observational fields over the United States, although the HRPPs have a shorter record for comparison.

NARR's diurnal cycle features a prominent nocturnal maximum over the midwestern United States, matching the pattern identified by Wallace (1975) and described as a pattern of propagating convective systems that initiate in the afternoon over the lee of the Rockies (e.g., Carbone et al. 2002). Similar nocturnal maxima are observed in association with other prominent mountain ranges, including for example in the lee of the Andes over Argentina (Laing and Fritsch 2000). Precipitation assimilation provides NARR with a diurnal cycle that is much improved over the global reanalysis. Some disagreements between NARR and the HRPPs persist, however, with the NARR diurnal cycle over the continental United States peaking slightly later in the nighttime. The extent of the nocturnal propagation in NARR also extends much farther into the Northeast and Pacific Northwest.

Large differences emerge outside of the continental United States, where assimilated diurnal precipitation was not observationally resolved. Consistent afternoon convection dominates over western Canada, Alaska, and Mexico; a diurnal cycle likely imposed by the quick trigger of the global reanalysis model's simplified Arakawa–Schubert convective scheme (Pan and Wu 1995). Propagating systems penetrate into the southern Canadian plains during the nighttime, apparently initiated in the afternoon over the United States. The diurnal cycle in eastern Canada is quite puzzling, as this area shows a very different phase in NARR than the global reanalysis' afternoon maximum generated from shorter R2 forecasts, and even CMORPH and PERSIANN differ in this region's diurnal phase. Bukovsky and Karoly (2007) also note the appearance of spurious rainfall events in eastern Canada. It is possible that the better representation of Midwest convection in NARR uniquely conditions air masses flowing into this region, but further

investigation is required. Precipitation assimilation also seems to decrease the diurnal amplitude (along with mean totals) over the oceans in comparison to the areas north of 42.5°N, and the morning peak seen over the Gulf Stream in the HRPPs and global reanalysis disappears.

b. Normalized covariances

Water cycle component interactions leading to precipitation on the diurnal time scale are shown as normalized covariances in Fig. 4. Interactions with assimilated precipitation (P'), which show the final patterns of behavior recorded in NARR output, are shown in Figs. 4a–d. Interactions with the model precipitation estimate (M'), which estimate the internal patterns of behavior of the model before precipitation assimilation occurs, are presented in Figs. 4a–d. In addition to analysis of the NARR behavior patterns, comparisons between the two columns reveal the adjustments made to the water cycle by precipitation assimilation.

Normalized covariances describing the exchange of evaporation and assimilated precipitation show remarkably stark U.S. borders and coastlines (Fig. 4a). Diurnal evaporation and precipitation do not strongly exchange in any direct fashion over much of the United States, although evaporation contributes slightly to diurnal rainfall over the western mountains and Gulf coast. Areas with nocturnal precipitation maxima have strongly negative normalized diurnal covariances with evaporation, showing that rain falls out of phase from the solar forcing that drives evaporation. In western Canada, diurnal precipitation dominantly exchanges with evaporation, which varies to a greater extent than precipitation during the day over the Rockies and the Mackenzie Mountains. This suggests a localized thermodynamic trigger to NARR's afternoon convection in this region possibly imposed through the use of the R2's diurnal cycle in precipitation assimilation. Precipitation and evaporation show no direct covariant relationship on the diurnal scale in the southern Canadian plains. Over Mexico, evaporation provides a small contribution to the diurnal rainfall, but does not appear to be a dominant driver. A lack of diurnally varying sea surface temperature negates a strong diurnal signal to marine evaporation.

Normalized covariances describing the exchange of moisture from moisture flux convergence to assimilated precipitation are shown in Fig. 4b. Becker et al. (2009) have previously shown a strong relationship between moisture flux convergence and daily precipitation maxima in NARR. As was identified in RR2008, there is a strong supply of moisture provided from the Gulf of Mexico by the low-level jet (LLJ) that tracks propagating storms across the nocturnal maximum region of the Midwest (Higgins et al. 1997). This circulation (explored also in Ruane and Roads 2007a) provides for a relatively moist continental interior at midlatitudes, a feature that is unique to North America. Moisture flux convergence seems to largely explain the diurnal timing of the summertime precipitation in this region, although its interaction with lagged moisture inputs is discussed below. A strong normalized diurnal covariance relationship between the assimilated precipitation and dynamical convergence also points to a strong land–sea circulation pattern that delivers moisture for precipitation over the East Coast and Florida. NARR's moisture flux convergence plays a small role in the diurnal precipitation over Canada, but over Mexico the North American monsoon provides strong diurnal moisture flux convergence that greatly exceeds the assimilated diurnal precipitation, as the background environment is far below saturation. Precipitation in the warm and nearly saturated air over the Gulf of Mexico and Gulf Stream also reacts strongly to diurnal variations in moisture flux convergence.

The strong negative covariant relationship between the assimilated precipitation and a declining precipitable water tendency throughout most of the NARR domain reflects the afternoon maximum in precipitation that on most days corresponds to the hours of peak evaporation (Fig. 4c). Thus, evaporation normally increases the moisture content of the atmospheric water column at the same time as precipitation occurs on other days. Over land, the lone exception to this feature occurs over the nocturnal precipitation maximum region that extends from the Midwest eastward to New England. In this area, afternoon evaporation loads the precipitable water column, providing plentiful moisture to be converted to rainfall as propagating storms pass through overnight. Thus, a lagged recycling of evaporated moisture is captured here, forming a distinct diurnal footprint of propagating convection. This feature is strongly affected by the Canadian border, but a signature appears to push across the border between assimilation times. Lingering convection also appears to erode the water column during the nighttime over the Pacific Northwest, where the Cascades may be mimicking the role of the Rockies in the upper Midwest.

The normalized covariance of the diurnal residual error term and the assimilated precipitation (Fig. 4d) shows where the water budget is unbalanced on the diurnal time scale. In areas where this term is large, the NARR modeling system is confronted by water budget imbalances relating to reinitializations and/or precipitation assimilation that may be comparable in diurnal magnitude to evaporation, moisture flux convergence, or precipitable water tendency. These imbalances are generally linked to physical characteristics of the regional geography and

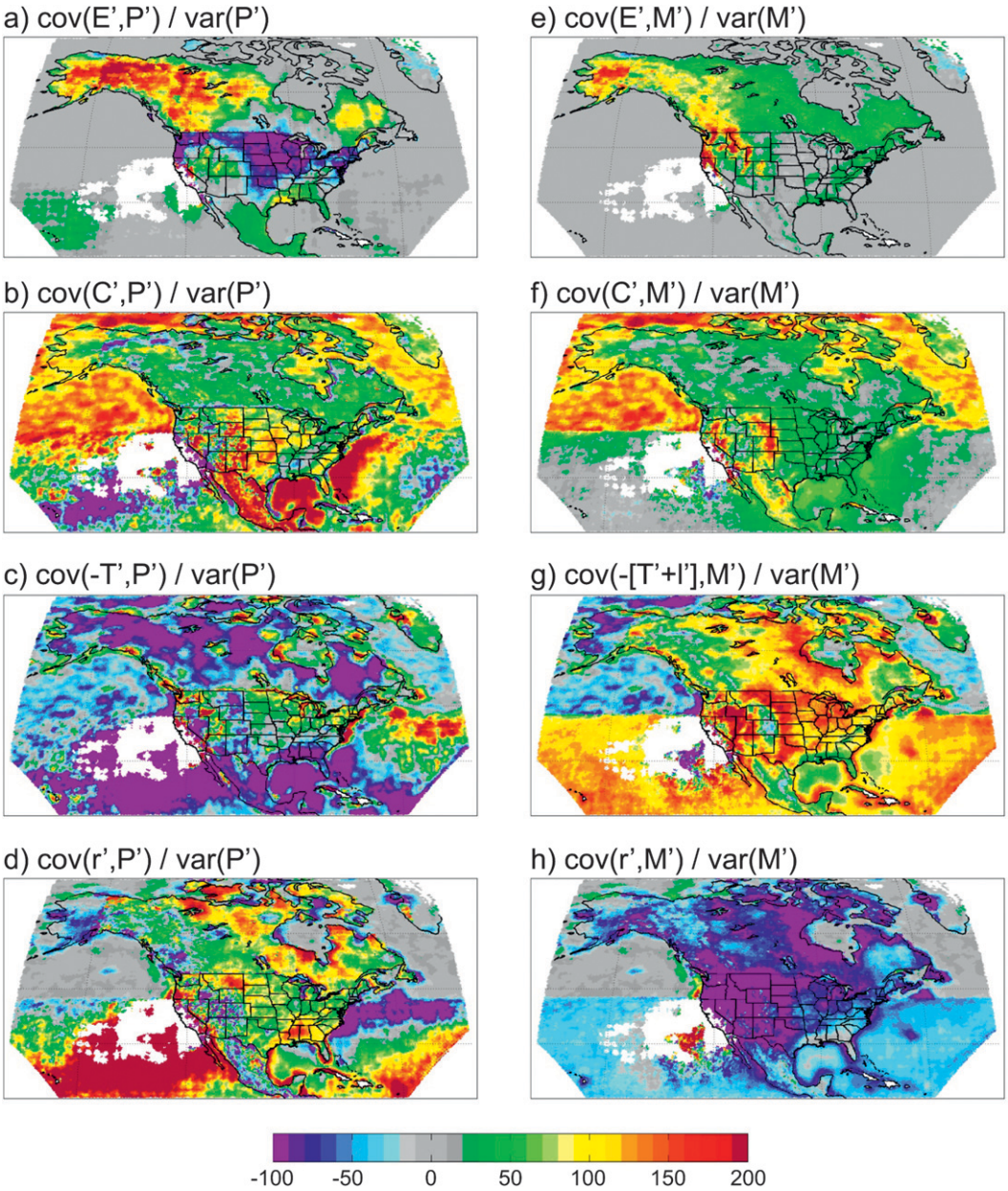

FIG. 4. The 1980–99 summertime mean normalized covariances (%) of diurnal precipitation with each of the other water cycle components for (a)–(d) assimilated precipitation and (e)–(h) model precipitation. Each row shows the normalized covariance of precipitation with (a),(e) evaporation, (b),(f) moisture flux convergence, (c),(g) precipitable water tendency, and (d),(h) the water budget residual for the column. The sum of the four panels in each column therefore explains 100% of the (assimilated or model) precipitation according to Eqs. (7a) and (7b), and the areas with the lowest 5% of the diurnal variance are omitted.

climate, which may help NARR users account for imbalances and will aid in the development of future reanalyses. For example, the analysis increment is expected to show prominent errors over complex mountains and coastlines, while precipitation assimilation is a likely culprit behind imbalances over the low-rainfall regions of the eastern Pacific, the morning precipitation maximum over eastern Canada, and the northern edge of the Gulf Stream.

A comparison with normalized covariances describing the model precipitation estimate through interaction with other water cycle components reveals the value added by precipitation assimilation. Before precipitation assimilation, there was no nocturnal maximum in

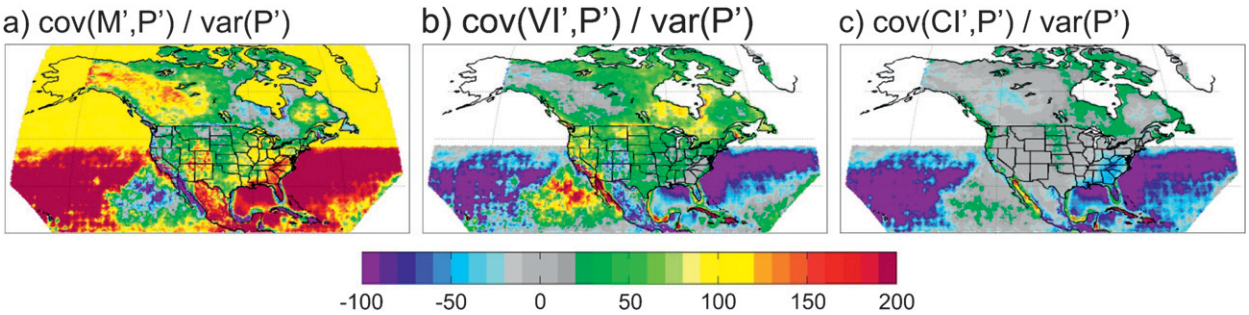

FIG. 5. The 1980–99 summertime mean normalized covariances (%) of the diurnal assimilated precipitation with each of its components: (a) model precipitation, (b) water vapor assimilation increments, and (c) liquid water assimilation increments. The sum of the three panels therefore explains 100% of the assimilated precipitation according to Eqs. (3), (7a), and (7b). Note that the white areas in (b) and (c) did not undergo precipitation assimilation.

precipitation (Fig. 4e) and little connection between the LLJ and convective storms in the Midwest (Fig. 4f). Normalized diurnal covariances of evaporation and the model precipitation estimate over western Canada are much closer to 100% than they were for assimilated precipitation. Similarly, diurnal moisture flux convergence variation does not exceed the model precipitation estimate over Mexico or the warm Atlantic coastal waters. The reduction in normalized covariances exceeding 100% in both plots reflects that precipitation assimilation in these areas has reduced the diurnal variation of precipitation to match the observations without a comparable reduction in the diurnal variation of evaporation or moisture flux convergence, underscoring that the diurnal variation of these variables in NARR output is likely overstated in many regions.

Figures 4g and 4h reveal how the diurnal cycle is imposed by precipitation assimilation. On a diurnal scale, when NARR's underlying model produces erroneous precipitation (according to the assimilated precipitation sets), the precipitation assimilation scheme removes that precipitation (M') and additional moisture ($-I'$) to relieve pressure on the convective parameterizations. Thus, we see a shift in the diurnal phase occurring where the normalized covariance of the column moisture terms with the model precipitation estimate is strongly positive in Fig. 4g. This is most striking in the imposition of the nocturnal maximum over the upper Midwest and the morning precipitation maximum over eastern Canada. After separating out the assimilation increment, the normalized covariances of the residual error term (primarily the analysis increment) and the model precipitation estimate (Fig. 4h) are almost entirely negative, indicating that reinitialization finds a discrepancy in the atmospheric moisture inversely related to the diurnal cycle of the precipitation in the underlying model.

To further understand the role of precipitation assimilation on the diurnal water balance, Fig. 5 presents the normalized covariances describing the precipitation through its assimilation components [combining Eqs. (1) and (3) and evaluating in the manner of Eq. (7)]. In contrast to the annual time scale, where the model precipitation estimate had a common phase but greater magnitude of variation than the assimilated precipitation (Part I), precipitation assimilation causes more drastic changes to the diurnal precipitation. Figure 5a shows many regions where the precipitation assimilation has adjusted the phase of the diurnal rainfall (resulting in low normalized covariances between M' and P'), and in places with consistent phases there are shifts in the amplitude of the diurnal variation. The model precipitation is still overactive over the oceans, Mexico, portions of western Canada, and the southeast United States, but over a large part of the continent there is a large contribution from the precipitation assimilation increment terms. The larger contribution from the vapor increment term suggests that precipitation assimilation requires adjustments to the relative humidity profile more than changes to the cloud profile. Over Mexico, the magnitude of the diurnal precipitation is reduced with corrections to the water column coming mainly in lower relative humidities. In contrast, reductions in diurnal rainfall over the southeast United States and western Canada are imposed along with reductions to cloud layers generated by the model and without large changes in the overall relative humidities. Over the oceans, both water vapor and condensed water are removed to moderate the diurnal rainfall variation.

6. Summary, discussion, and future work

This study examined summertime balances and exchanges of the 1980–99 NARR atmospheric water cycle components in their long-term averages and on the diurnal time scale, establishing a summertime NARR hydroclimatology revealing distinct regional balances and component interactions largely constrained by the

assimilation of observed precipitation during this convective season. There are many intriguing features in the figures presented; although it is beyond the scope of this study to comprehensively explore them all, analyses are provided here in the interest of motivating continuing studies.

Several spurious features result from the assimilation of differing (in temporal and spatial resolution) observational rainfall datasets. The effects of the precipitation assimilation scheme were therefore explored to aid in the interpretation of NARR output for process studies, applications, and impacts assessments using an estimate of the precipitation and the water cycle of NARR's underlying Eta Model prior to precipitation assimilation. In most regions precipitation assimilation results in a reduction of the model precipitation; however, the other flux components (evaporation and moisture flux convergence) are not similarly adjusted. This overactive hydrologic cycle is occasionally out of step from the assimilated precipitation, resulting, for example, in a negative P–E relationship over many land areas and in slightly out-of-phase diurnal variations. Comparisons of the water cycle interaction of the underlying model and the assimilated output provide context for NARR's biases. The implementation of an ambitious precipitation assimilation scheme provides tremendous value to the NARR output, constraining one of the most important variables over North America despite these secondary effects. If these artifacts are considered, NARR holds great potential for process studies, applications, and impacts assessments (particularly over the continental United States where observational data are most complete), as the careful accounting of assimilation increments sheds light on the nature of these biases.

Results from Part I show that annual precipitation peaks in the thermodynamically active summertime over much of the continent, but the diurnal variation on top of this higher baseline shows a variety of dynamic process interactions. Alternatively, over the southeast United States, where seasonal moisture convergence is most closely related with the rainfall maximum, summertime diurnal rainfall is most closely related to local thermodynamic instability. These interactions underscore the ways in which the water cycle may act according to independent driving mechanisms on different frequencies.

NARR's diurnal cycle captures many of the complex diurnal characteristics over North America that are often lacking in other models and reanalysis systems, including the nocturnal rainfall maximum over the midwestern United States. This diurnal cycle is largely imposed on a modeling system that does not capture complex diurnal characteristics by the precipitation assimilation scheme, leaving evaporation and moisture flux convergence with mismatched diurnal phases and magnitudes likely compensated by strange patterns of behavior in the boundary layer. The timing of NARR's nocturnal rainfall maximum is slightly later than that produced by the satellite-based products.

Precipitation assimilation is therefore directly responsible for the presence in NARR of a nocturnal rainfall maximum in the upper Midwest, allowing for a more comprehensive examination of moisture transfer among water cycle components leading to this important rainfall feature. As the sun rises in the sky, the Rockies act as an elevated heating source that sets up a large-scale mountain-lowland circulation pattern with subsidence over the Great Plains—inhibiting convection during the afternoon when evaporation moistens the lower atmosphere. Moist instabilities and mountain waves initiate convection in rising air over the lee of the Rockies, propagating to the east over the upper Midwest under favorable amounts of vertical wind shear (Weisman and Rotunno 2004). Convective inhibition ends as night falls and propagating storms move over the Midwest, allowing storms to access built-up convective available potential energy (CAPE) and moisture in the water column with often spectacular storms. The moisture supply for these storms is partially sustained by the low-level jet that follows lines of convection across the continent, aiding in the setup of convective ''corridors'' for intense storms at the terminus of the LLJ (Tuttle and Davis 2006). Summertime convection therefore has many complex interactions that are a challenge to modelers, and each may be sensitive to large-scale climate changes.

The behavior of propagating nighttime storms is neatly summarized in the normalized covariance plots shown in Fig. 4. The moisture supplied to precipitation from coinciding diurnal variations of evaporation, moisture flux convergence, and precipitable water storage may be relatively compared for the average summertime evening across the region (recall that the diurnal variations are not the exclusive source of rainfall, existing on top of a seasonal baseline, for example). Discontinuities in the observational sources of assimilated precipitation disrupt these behavior patterns at the U.S. border, but it is likely that the upper midwestern systems extend into those locations in southern Canada where rainfall peaks at night. The morning peak of rainfall over eastern Canada in NARR stands out as a potential artifact not observed by the satellite products, and the substantial roles of the analysis and assimilation increment terms suggest that continued improvement in the underlying model will improve the comprehensive representation of the water cycle.

Many aspects of these evaluations merit further study, including unique regional behavior patterns and the

sensitivity of these relationships to interannual variation and climate change. Interesting diurnal patterns of behavior include a morning maximum in rainfall over the Ozarks that is detected by both high-resolution precipitation products but is absent from NARR, propagating convection in Arizona and northern Mexico possibly associated with a low-level jet leading out of the Gulf of California, and a later rainfall peak over the Carolinas relative to other southeastern states. NARR's performance may also be placed in context through comparison with other models, reanalyses (particularly those with precipitation assimilation), and observational products. Examinations of the water cycle component interactions in future climate scenarios are planned to identify potential sensitivities and regime shifts, and an investigation of the anomalous interactions associated with the 1988 drought and 1993 flood has revealed divergent nocturnal propagation patterns during the drought and the opposite during the flood. As remotely sensed global evaporation products continue to be developed, normalized covariance studies using nearly comprehensive observational water cycle products may be used to characterize natural processes and identify lingering biases.

Acknowledgments. This research was supported by an appointment to the NASA Postdoctoral Program at the Goddard Institute for Space Studies, administered by Oak Ridge Associated Universities (ORAU) through a contract with NASA. The views expressed herein are those of the author and do not necessarily reflect the views of NASA or ORAU. The author would like to thank Ernesto Hugo Berbery and Fedor Mesinger for early discussions about NARR's water cycle, Ying Lin for extensive assistance in revisiting NARR's precipitation assimilation scheme, Perry Shafran and Wesley Ebisuzaki for insight into the sources of precipitation assimilation, Radley Horton for multiple edits, Masao Kanamitsu for helpful advice, and anonymous reviewers of this manuscript. Anonymous reviewers of Part I were also helpful in shaping the tone and structure of this companion article.

REFERENCES

Anderson, B., A. C. Ruane, J. O. Roads, and M. Kanamitsu, 2009: Estimating the influence of evaporation and moisture-flux convergence upon seasonal precipitation rates. Part II: An analysis for North America based upon the NCEP–DOE Reanalysis II model. *J. Hydrometeor.,* **10,** 893–911.

Becker, E. J., and E. H. Berbery, 2008: The diurnal cycle of precipitation over the North American monsoon region during the NAME 2004 field campaign. *J. Climate,* **21,** 771–787.

——, ——, and R. W. Higgins, 2009: Understanding the characteristics of daily precipitation over the United States using the North American Regional Reanlaysis. *J. Climate,* **22,** 6268–6286.

Black, T. L., 1994: The new NMC mesoscale Eta Model: Description and forecast samples. *Wea. Forecasting,* **9,** 265–278.

Bukovsky, M. S., and D. J. Karoly, 2007: A brief evaluation of precipitation from the North American Regional Reanalysis. *J. Hydrometeor.,* **8,** 837–846.

Carbone, R. E., J. D. Tuttle, D. A. Ahijevych, and S. B. Trier, 2002: Inferences of predictability associated with warm season precipitation episodes. *J. Atmos. Sci.,* **59,** 2033–2056.

Changnon, S. A., 2001: Thunderstorm rainfall in the conterminous United States. *Bull. Amer. Meteor. Soc.,* **82,** 1925–1940.

Dai, A., 2001: Global precipitation and thunderstorm frequencies. Part II: Diurnal variations. *J. Climate,* **14,** 1112–1128.

——, and K. E. Trenberth, 2004: The diurnal cycle and its depiction in the Community Climate System Model. *J. Climate,* **17,** 930–951.

——, F. Giorgi, and K. E. Trenberth, 1999: Observed and model-simulated diurnal cycles of precipitation over the contiguous United States. *J. Geophys. Res.,* **104,** 6377–6402.

——, X. Lin, and K. Hsu, 2007: The frequency, intensity, and diurnal cycle of precipitation in surface and satellite observations over low- and mid-latitudes. *Climate Dyn.,* **29,** 727–744, doi:10.1007/s00382-007-0260-y.

Dirmeyer, P. A., and K. L. Brubaker, 2007: Characterization of the global hydrologic cycle from a back-trajectory analysis of atmospheric water vapor. *J. Hydrometeor.,* **8,** 20–37.

Ek, M. B., K. E. Mitchell, Y. Lin, E. Rogers, P. Grunmann, V. Koren, G. Gayno, and J. D. Tarpley, 2003: Implementation of Noah land surface model advances in the National Centers for Environmental Prediction operational mesoscale Eta Model. *J. Geophys. Res.,* **108,** 8851, doi:10.1029/2002JD003296.

Fritsch, J. M., R. J. Kane, and C. R. Chelius, 1986: The contribution of mesoscale convective weather systems to the warm-season precipitation in the United States. *J. Climate Appl. Meteor.,* **25,** 1333–1345.

Higgins, R. W., Y. Yao, E. S. Yarosh, J. E. Janowiak, and K. C. Mo, 1997: Influence of the Great Plains low-level jet on summertime precipitation and moisture transport over the central United States. *J. Climate,* **10,** 481–507.

——, W. Shi, E. Yarosh, and R. Joyce, 2000: Improved U.S. precipitation quality control system and analysis. *NCEP/Climate Prediction Center Atlas,* NOAA/NWS Atlas 7, 40 pp.

Hsu, K., X. Gao, S. Sorooshian, and H. V. Gupta, 1997: Precipitation estimation from remotely sensed information using artificial neural networks. *J. Appl. Meteor.,* **36,** 1176–1190.

Janjić, Z. I., 1994: The step-mountain Eta coordinate model—Further developments of the convection, viscous sublayer, and turbulence closure schemes. *Mon. Wea. Rev.,* **122,** 927–945.

Joyce, R. J., J. E. Janowiak, P. A. Arkin, and P. Xie, 2004: CMORPH: A method that produces global precipitation estimates from passive microwave and infrared data at high spatial and temporal resolution. *J. Hydrometeor.,* **5,** 487–503.

Kanamaru, H., and M. Kanamitsu, 2007: Fifty-seven-year California Reanalysis Downscaling at 10 km (CaRD10). Part II: Comparison with North American Regional Reanalysis. *J. Climate,* **20,** 5572–5592.

Kanamitsu, M., W. Ebisuzaki, J. Woollen, S.-K. Yang, J. Hnilo, M. Fiorino, and J. Potter, 2002: NCEP–DOE AMIP-II Reanalysis (R-2). *Bull. Amer. Meteor. Soc.,* **83,** 1631–1643.

Laing, A. G., and J. M. Fritsch, 2000: The large-scale environments of the global populations of mesoscale convective complexes. *Mon. Wea. Rev.,* **128,** 2756–2776.

Lin, Y., K. E. Mitchell, E. Rogers, M. E. Baldwin, and G. I. DiMego, 1999: Test assimilations of the real-time, multi-sensor hourly precipitation analysis into the NCEP Eta model. Preprints, *Eighth Conf. on Mesoscale Meteorology,* Boulder, CO, Amer. Meteor. Soc., 314–344.

Mearns, L. O., W. Gutowski, R. Jones, R. Leung, S. McGinnis, A. Nunes, and Y. Qian, 2009: A regional climate change assessment program for North America. *Eos, Trans. Amer. Geophys. Union,* **90,** 311.

Mesinger, F., and Coauthors, 2006: North American Regional Reanalysis. *Bull. Amer. Meteor. Soc.,* **87,** 343–360.

Mo, K. C., M. Chelliah, M. L. Carrera, R. W. Higgins, and W. Ebisuzaki, 2005: Atmospheric moisture transport over the United States and Mexico as evaluated in the NCEP Regional Reanalysis. *J. Hydrometeor.,* **6,** 710–728.

Nakamura, K., 2004: Diurnal variation of precipitation measured by the TRMM TMI. *GEWEX Newsletter,* Vol. 14, No. 2, International GEWEX Project Office, Silver Spring, MD, p. 4. [Available online at http://www.gewex.org/May2004.pdf.]

Nigam, S., and A. Ruiz-Barradas, 2006: Seasonal hydroclimate variability over North America in global and regional reanalyses and AMIP simulations: Varied representation. *J. Climate,* **19,** 815–837.

Pan, H.-L., and L. Mahrt, 1987: Interaction between soil hydrology and boundary layer developments. *Bound.-Layer Meteor.,* **38,** 185–202.

——, and W.-S. Wu, 1995: Implementing a mass flux convection parameterization package for the NMC Medium-Range Forecast Model. NMC Office Note 409, 40 pp. [Available from NCEP/EMC 5200 Auth Rd., Camp Springs, MD 20746.]

Rogers, E., M. Ek, Y. Lin, K. Mitchell, D. Parrish, and G. DiMego, cited 2009: Changes to the NCEP Meso Eta analysis and forecast system: Assimilation of observed precipitation, upgrades to land-surface physics, modified 3DVAR analysis. NOAA/NCEP/EMC. [Available online at www.emc.ncep.noaa.gov/mmb/mmbpll/spring2001/tpb.]

Ruane, A. C., 2010: NARR's atmospheric water cycle components. Part I: 20-year mean and annual interactions. *J. Hydrometeor.,* **11,** 1205–1219.

——, and J. O. Roads, 2007a: The diurnal cycle of water and energy over the continental United States from three reanalyses. *J. Meteor. Soc. Japan,* **85A,** 117–143.

——, and ——, 2007b: 6-hour to 1-year variance of five global precipitation sets. *Earth Interactions,* **11.** [Available online at http://EarthInteractions.org.]

——, and ——, 2008: Dominant balances and exchanges of the atmospheric water cycle in the Reanalysis 2 at diurnal, annual, and intraseasonal time scales. *J. Climate,* **21,** 3951–3966.

Schubert, S., and Y. Chang, 1996: An objective method for inferring sources of model error. *Mon. Wea. Rev.,* **124,** 325–340.

Shafran, P., J. Woollen, W. Ebisuzaki, W. Shi, Y. Fan, R. Grumbine, and M. Fennessy, 2004: Observational data used for assimilation in the NCEP North American Regional Reanalysis. Preprints, *14th Conf. on Applied Climatology,* Seattle, WA, Amer. Meteor. Soc., 1.4. [Available online at http://ams.confex.com/ams/pdfpapers/71689.pdf.]

Trenberth, K. E., A. Dai, R. M. Rasmussen, and D. B. Parsons, 2003: The changing character of precipitation. *Bull. Amer. Meteor. Soc.,* **84,** 1205–1217.

Tuttle, J. D., and C. A. Davis, 2006: Corridors of warm season precipitation in the central United States. *Mon. Wea. Rev.,* **134,** 2297–2317.

Wallace, J. M., 1975: Diurnal variations in precipitation and thunderstorm frequency over the conterminous United States. *Mon. Wea. Rev.,* **103,** 406–419.

Wang, S.-Y., and T.-C. Chen, 2009: The late-spring maximum of rainfall over the U.S. central plains and the role of the low-level jet. *J. Climate,* **22,** 4696–4709.

Weisman, M. L., and R. Rotunno, 2004: ''A Theory for Strong Long-Lived Squall Lines'' revisited. *J. Atmos. Sci.,* **61,** 361–382.

West, G. L., W. J. Steenburgh, and W. Y. Y. Cheng, 2007: Spurious grid-scale precipitation in the North American Regional Reanalysis. *Mon. Wea. Rev.,* **135,** 2168–2184.

Xie, P., and P. A. Arkin, 1997: Global precipitation: A 17-year monthly analysis based on gauge observations, satellite estimates, and numerical model outputs. *Bull. Amer. Meteor. Soc.,* **78,** 2539–2558.